The sensitivity of modal lines position for a chosen mode is very high in the case of multiple eigenvalues. For example, it was checked that the small distortion $\epsilon_0 = 0.9 \times 10^{-6}$ introduced only into element no. 24 reduces the local vibration due to the first mode (assuming $r = 1$) almost to zero. The corresponding nodal lines for the first two modes of vibration are shown in Figs. 2a and 2b, respectively (broken lines). As we can see, the effect of the shifting of the nodal line for the chosen mode (point B) to a certain point (point A) can be done easily.

Of course, the problem of simultaneous reduction of local vibration for the first two modes cannot be so effective. Assuming $r = 2$ and restricting considerations to the set $\mathfrak{A}$ of members from the lower layer (24 elements, nos. 43–66, cf. Fig. 1) as possible locations for actuators, the following optimal solution minimizing the objective function of Eq. (8) has been reached by the optimization procedure, with distortions in elements 43–66, respectively, given in the first row (denoted by ϵ_0) in Table 1.

The objective function was reduced to $u_{lm} = 0.9204$ (local vibration reduced by 15%). The nodal lines for two of the first, optimally shaped modes of vibration are shown (broken lines) in Figs. 3a and 3b, respectively. The gradient of goal function of Eq. (8) (calculated for the preceding solution) with respect to the control parameters takes the components shown in the second row (denoted by $\partial u_{lm}/\partial \epsilon_0$) in Table 1.

The products of the components of vectors ϵ_0 and $\partial u_{lm}/\partial \epsilon_0$ (a component-by-component check) take nonpositive values (with zero values for unconstrained components), so it can be proved that the Kuhn-Tucker stationary conditions are satisfied for the solution.

Concluding Remarks

A procedure for reducing vibration at sensitive locations on a structure by induced distortions was derived and demonstrated for an antenna truss example. It was shown that with repeated frequencies it is very easy to move nodal lines of one of the modes. For the more realistic problem of modifying both modes, it was still possible to obtain 15% reduction in amplitude with induced distortions limited to 0.4%.

In real applications an additional constraint may be to reduce the number of elements that contain length actuators. In such a case it may be important to locate the most effective elements first before proceeding to the optimization of the values of the induced distortions.

Acknowledgment

This work was supported in part by NASA Grant NAG-1-224.

References

[1]Taylor, R. B., "Helicopter Vibration Reduction by Rotor Blade Model Shaping," 38th Annual Forum of the American Helicopter Society, Paper A-82-38-09-3000, Anaheim, CA, May 1982.

[2]Taylor, R. B., "Helicopter Rotor Blade Design for Minimum Vibration," NASA CR-3825, Oct. 1984.

[3]Pritchard, J. I., Adelman, H. M., and Haftka, R. T., "Sensitivity Analyses and Optimization of Nodal Point Placement for Vibration Reduction," NASA TM-87763, July 1986.

[4]Crawley, E. G., and de Luis, J., "Use of Piezo-Ceramics as Distributed Actuators in Large Space Structures," *AIAA Journal*, Vol. 25, No. 10, 1987, pp. 1373–1385.

[5]Im, S. A, and Atluri, S. N., "Effects of Piezo-Actuators on a Finitely Deformed Beam Subjected to General Loading," *AIAA Journal*, Vol. 27, No. 12, 1989, pp. 1801–1807.

[6]Thareja, R., and Haftka, R. T., "NEWSUMT-A, A Modified Version of NEWSUMT for Inequality and Equality Constraints," Virginia Polytechnic Inst. and State Univ., Blacksburg, VA, March 1985.

Partial Hybrid Strip Model for Higher-Order Laminated Plate Theory

Yi-Ping Tseng* and Wei-Jer Wang†
Tamkang University, Taiwan 25137, Republic of China

Introduction

In the displacement-based model of classical plate theory, Mindlin theory, and higher-order theories, the essential problem is the interface traction discontinuity. The difficulty can be avoided by the hybrid stress method. However, the drawbacks are the complicated formulation and expensive computational cost. Based on the modified Hillinger-Reissner principle, a three-dimensional partial hybrid stress element has been developed by Jing and Liao.[1] The hybrid model is only partially used in transverse shear part; however, excellent accuracy and fast convergence are observed.

Although the finite strip method is limited to the ply orientation, its application in cross-ply and symmetrical angle-ply laminates greatly reduces the number of variables. The present study extends the finite strip method by using the higher-order plate theory, and the partial hybrid stress method is further incorporated. It is then called the partial hybrid strip model (PHSM). Quite accurate displacement results are obtained, and the through thickness stress distributions are also in fair agreement with the existing elasticity solution.

Partial Hybrid Strip Method

The displacement field of higher-order plate theory by Lo et al.[2] is adopted

$$\begin{aligned} u(x,y,z) &= u_0(x,y) + z\theta_y(x,y) + z^2 u^*(x,y) + z^3\theta_y^*(x,y) \\ v(x,y,z) &= v_0(x,y) + z\theta_x(x,y) + z^2 v^*(x,y) + z^3\theta_x^*(x,y) \\ w(x,y,z) &= w_0(x,y) + z\theta_z(x,y) + z^2 w^*(x,y) \end{aligned} \tag{1}$$

In the finite strip method, the midplane displacements are interpolated as

$$\begin{aligned} u_0 &= \sum_{i=1}^{\text{nst}} \sum_{m=1}^{r} Y_m(y) N_i(\xi) u_{0i}, \quad v_0 = \sum_{i=1}^{\text{nst}} \sum_{m=1}^{r} Y_m'(y) N_i(\xi) v_{0i} \\ w_0 &= \sum_{i=1}^{\text{nst}} \sum_{m=1}^{r} Y_m(y) N_i(\xi) w_{0i}, \quad \theta_x = \sum_{i=1}^{\text{nst}} \sum_{m=1}^{r} Y_m'(y) N_i(\xi) \theta_{xi} \\ \theta_y &= \sum_{i=1}^{\text{nst}} \sum_{m=1}^{r} Y_m(y) N_i(\xi) w_{0i}, \quad \theta_z = \sum_{i=1}^{\text{nst}} \sum_{m=1}^{r} Y_m(y) N_i(\xi) \theta_{zi} \\ u^* &= \sum_{i=1}^{\text{nst}} \sum_{m=1}^{r} Y_m(y) N_i(\xi) u_i^*, \quad v^* = \sum_{i=1}^{\text{nst}} \sum_{m=1}^{r} Y_m'(y) N_i(\xi) v_i^* \\ w^* &= \sum_{i=1}^{\text{nst}} \sum_{m=1}^{r} Y_m(y) N_i(\xi)_x w_i^*, \quad \theta_x^* = \sum_{i=1}^{\text{nst}} \sum_{m=1}^{r} Y_m'(y) N_i(\xi) \theta_{xi}^* \\ \theta_y^* &= \sum_{i=1}^{\text{nst}} \sum_{m=1}^{r} Y_m(y) N_i(\xi) \theta_{yi}^* \end{aligned} \tag{2}$$

where nst is the nodal number per strip, r the terms of series used, $Y_m(y)$ the eigenfunction, and $N_i(\xi)$ the interpolation functions between nodal lines.

Received May 13, 1991; revision received Sept. 4, 1991; accepted for publication Sept. 6, 1991.

*Assistant Professor, Department of Civil Engineering.
†Graduate Student, Department of Civil Engineering.

In the partial hybrid stress model,[1] the stress, strain, and material property are separated into flexural and transverse shear parts. These two parts represented by subscripts f and t are formulated by the displacement and hybrid models, respectively. However, the three-dimensional displacement field $\{u\}$ is interpreted by the midplane displacements $\{d\}$ herein. For the present partial hybrid strip model of n strips laminated of nl plies, the self-consistent modified Hellinger-Reissner functional π becomes

$$\pi=\sum_{i=1}^{n}\sum_{k=1}^{nl}\left[\int_{V_{ni}}\left(\frac{1}{2}([\bar{B}_f]\{d\})^t\{\sigma_f^k\}+\{\sigma_t^k\}^t([\bar{B}_t]\{d\})\right.\right.$$
$$\left.\left.-\frac{1}{2}\{\sigma_t^k\}^t[S_t^k]\{\sigma_t^k\}\right)dV-\int_{S\sigma_{ni}}\{u\}^t\{\bar{T}\}ds\right] \quad (3)$$

where V_{ni} is the volume of the ith strip, $S\sigma_{ni}$ the area in the ith strip subjected to transverse loading $\bar{T}$, and $[\bar{B}_f]$ and $[\bar{B}_t]$ are the proper differential operators.

The transverse shear stress field $\{\sigma_t\}$ is assumed as in the hybrid model:

$$\{\sigma_t^k\}=[P^k]\{\beta^k\} \quad (4)$$

where $[P^k]$ are polynomials and $\{\beta\}$ are stress parameters.

In the finite strip formulation, Eqs. (2) and (4) and plate stiffness are substituted into Eq. (3), π becomes

$$\pi=\sum_{i=1}^{n}\frac{1}{2}\{q\}^t[k_f]\{q\}+\sum_{i=1}^{n}[\{\beta\}^t[G]\{q\}-\frac{1}{2}\{\beta\}^t[H]\{\beta\}$$
$$-\sum_{i=1}^{n}\{q\}^t\{Q\}$$

where the flexural strip stiffness $[k_f]$ is the same as the displacement model, and $[G]$ and $[H]$ are standard symbols in the hybrid model.[3]

Taking variation with respect to $\{\beta\}$ and then $\{q\}$, we obtain the equation for each strip as

$$[k]\{q\}-\{Q\}=0 \quad (6)$$

with the strip stiffness matrix being

$$[k]=[k_f]+[k_t] \quad (7)$$

where the transverse shear strip stiffness $[k_t]=[G]^t[H]^{-1}[G]$ is the same as the hybrid model.

Flexural stresses are computed as in the displacement model, whereas transverse shear stresses are evaluated by the hybrid model.

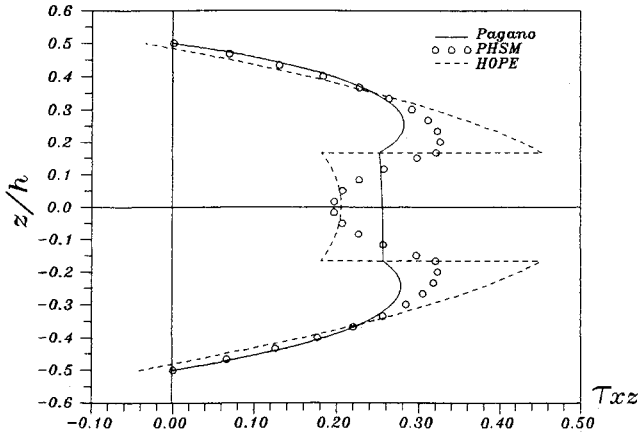

Fig. 1 Distribution of $\bar{\tau}_{xz}$ (0, $a/2$, z/h) for (0/90/0 deg) $a/h=4$ plate.

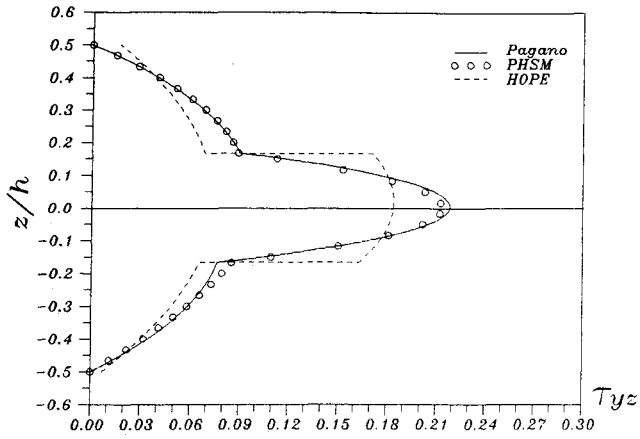

Fig. 2 Distribution of $\bar{\tau}_{yz}$ ($a/2$, 0, z/h) for (0/90/0 deg) $a/h=4$ plate.

Assumed Transverse Shear Stress Field

The $[P]$ polynomials include $(1, z, z^2)$ terms due to the plate displacement field and $[\sin(m\pi y/b)(1,x,x^2), \cos(m\pi y/b)(1,x,x^2)]$ terms due to the interpolation functions. After layer assembly process has been imposed and traction boundary conditions on surfaces and interfaces are enforced, the three-layered plates yield

$$\tau_{xz}{}^i=[P_x^i]\{\beta_x^i\}, \qquad \tau_{yz}{}^i=[P_y^i]\{\beta_y^i\}$$

where

$[P_x^1]$: $(1-4z^2/h^2)S(1,x,x^2)$, $(z+2z^2/h)S(1,x,x^2)$

$[P_y^1]$: $(1-4z^2/h^2)C(1,x,x^2)$, $(z+2z^2/h)C(1,x,x^2)$

$[P_x^2]$: $(32z^2/h^2)S(1,x,x^2)$, $(z-4z^2/h^2)S(1,x,x^2)$

$(1-36z^2/h^2)S(1,x,x^2)$, $(z+6z^2/h)S(1,x,x^2)$

$[P_y^2]$: $(32z^2/h^2)C(1,x,x^2)$, $(-4z^2/h)C(1,x,x^2)$

$(1-36z^2/h^2)C(1,x,x^2)$, $(z+6z^2/h)C(1,x,x^2)$

$[P_x^3]$: $(8z/h-16z/h^2)S(1,x,x^2)$, $(2z^2/h-z)S(1,x,x^2)$

$(3z-6z^2/h)S(1,x,,x^2)$

$(1-8z/h+12z^2/h^2)S(1,x,x^2)$

$[P_y^3]$: $(8z/h-16z^2/h^2)C(1,x,x^2)$, $(2z^2/h-z)C(1,x,x^2)$

$(3z-6z^2/h)C(1,x,,x^2)$

$(1-8z/h+12z^2/h^2)C(1,x,x^2)$

$\{\beta_x^1\}$: $\{\beta_1-\beta_6\}^t$

$\{\beta_y^1\}$: $\{\beta_{16}-\beta_{51}\}^t$

$\{\beta_x^2\}$: $\{\beta_1-\beta_{12}\}^t$

$\{\beta_y^2\}$: $\{\beta_{16}-\beta_{27}\}^t$

$\{\beta_x^3\}$: $\{\beta_1-\beta_6, \beta_{10}-\beta_{15}\}^t$

$\{\beta_y^3\}$: $\{\beta_{16}-\beta_{21}, \beta_{25}-\beta_{30}\}^t$

with $S=\sin(m\pi y/b)$, $C=\cos(m\pi y/b)$, and b being the width.

Numerical Examples

Two typical examples with elasticity solution of Pagano[4] are illustrated. Cross-ply (0/90/0 deg) and (0/90 deg) square

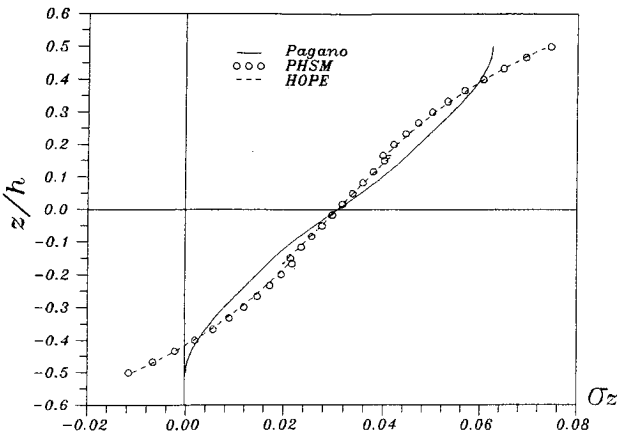

Fig. 3 Distribution of $\bar{\sigma}_z$ ($a/2$, $a/2$, z/h) for (0/90/0 deg) $a/h = 4$ plate.

composite plates are subjected to sinusoidal loading. Both examples are simply supported and of the same thickness per ply. Various span-to-thickness (a/h) ratios are investigated. The full plate is divided into 2, 6, and 10 strips, and one term of $Y_m(y)$ series is used because of only one term in sinusoidal loading.

The displacement analysis of the present model is more accurate than those of Kant and Pandya[5] and the refined C^1 higher-order plate theory of Reddy[6] in these examples. It is thought to be attributed to the overcome interlaminar traction discontinuity.

Both the present PHSM and the higher-order plate element[5] (HOPE) closely predict the through thickness variation of in-plane deformation $\bar{u}$ and the flexural stresses ($\bar{\sigma}_x$, $\bar{\sigma}_y$, $\bar{\tau}_{xy}$, $\bar{\sigma}_z$). The $\bar{\tau}_{xz}$, $\bar{\tau}_{yz}$, $\bar{\sigma}_z$ for $a/h = 4$ (0/90/0 deg) plates are shown in Figs. 1-3. The PHSM can yield a rational distribution of ($\bar{\tau}_{xz}$, $\bar{\tau}_{yz}$) satisfying traction boundary conditions. The $\bar{\tau}_{yz}$ is in excellent agreement with the exact solution[4]. There exists deviation of $\bar{\tau}_{xz}$, however, it is continuous through thickness. On the other hand, obvious discontinuity is observed in HOPE. The continuity of $\bar{\sigma}_z$ is neglected since the transverse shear stress is more significant. Therefore, the present formulation becomes straightforward, whereas self-equilibrating stress fields are not required herein.

Conclusions

The hybrid model is adopted partially in the present model. Therefore, acceptable through thickness transverse shear stress variations are obtained. As the through thickness effect is closely predicted, excellent accuracy and fast convergence are observed for the cross-ply laminates. The computational cost is enormously reduced because of the finite strip method, and only transverse shear stress parameters are required.

References

[1]Jing, H. S., and Liao, M. L., "Partial Hybrid Stress Element for the Analysis of Thick Laminated Composite Plates," *International Journal for Numerical Methods in Engineering*, Vol. 28, No. 12, 1989, pp. 2813-2827.

[2]Lo, K. H., Christensen, R. M., and Wu, E. M., "A Higher-Order Theory of Plate Deformation Part 2: Laminated Plates," *Journal of Applied Mechanics*, Vol. 44, No. 4, 1977, pp. 669-676.

[3]Spilker, R. L., "Invariant 8-Node Hybrid Stress Elements for Thin and Moderately Thick Plates," *International Journal for Numerical Methods in Engineering*, Vol. 18, No. 3, 1982, pp. 1153-1178.

[4]Pagano, N. J., "Exact Solutions for Rectangular Bidirectional Composites and Sandwich Plates," *Journal of Composite Materials*, Vol. 4, No. 1, 1970, pp. 20-34.

[5]Kant, T., and Pandya, B. N., "A Simple Finite Element Formulation of a Higher-Order Theory for Unsymmetrically Laminated Composite Plates," *Composite Structures*, Vol. 9, 1988, pp. 215-246.

[6]Reddy, J. N., "On Refined Computational Models of Composite Laminates," *International Journal for Numerical Methods in Engineering*, Vol. 27, No. 2, 1989, pp. 361-382.

Approximate Vibrational Analysis of Noncircular Cylinders Having Varying Thickness

V. Kumar* and A. V. Singh†
University of Western Ontario,
London, Ontario N6A 5B9, Canada

Introduction

NONCIRCULAR cylindrical shells have been used in many industrial applications like flight and submarine structures. However, they have received little attention in the area of vibration and stability. The majority of the shell literature published is concerned with circular cylinders, and only a few deal with noncircular cylinders.[1] The variable curvature in noncircular cylinders introduces variable coefficients into their governing differential equations and causes their solution to be difficult. Hence most of the closed-form solutions presented in the literature use simplifying assumptions.

The purpose of the present study is to present an approximate free vibrational analysis for noncircular cylindrical shells having variable thickness along the circumference. In the present work the finite strip method is used since this method makes use of the regular geometry in the longitudinal direction and thereby reduces the size of the problem. A combination of polynomial and harmonic functions that satisfy the boundary conditions is used to represent the displacement components. Numerical results are presented for several oval cylindrical shells, and good comparisons are obtained with those available in the literature.

Analysis

The present analysis is applicable to homogenous, isotropic, elastic, thin-walled, cylindrical shells. The coordinate system and shell geometry are shown in Fig. 1. The bounding surfaces of the shell are assumed to be at distances $z = \pm h/2$ from the middle surface, where h is the wall thickness of the shell. The thickness of the shell at any point along the circumference is given by $h = h_0 H(s)$, where h_0 is the thickness at $s = 0$ and $H(s)$ is a prescribed function of s. Consistent with the assumptions of thin-shell theory, the thickness is considered to be small in comparison with the other characteristic dimensions of the middle surface.

The kinematic relations used in the present study are based on the Kirchhoff-Love assumptions of classical thin-shell theory, and the final equation of motion is derived with the aid of strain-displacement relations obtained by the simplification of the exact relations developed by Flügge.[2] The axial, circumferential, and radial displacement components of the middle surface are denoted by u^*, v^*, and w^*, respectively (Fig. 1). The displacements (u^*, v^*, and w^*), the axial and circumferential coordinates (x^* and s^*), and the radius of curvature (r^*) are cast into a nondimensionalized form given by $(u, v, w) = (u^*, v^*, w^*)/h_0$ and $(x,s,r) = (x^*, s^*, r^*)/r_0$. The quantity r_0 is defined as the average radius of the noncircular cylindrical shell and is given by $L_s/2\pi$, where L_s is the circumference of the middle surface. The simplified strain-displacement relations, in terms of the nondimensionalized parameters, are given by

$$\epsilon_x = u_{,x} - zw_{,xx}$$
$$\epsilon_s = v_{,s} + (w/r) - zw_{,ss} \qquad (1)$$
$$\epsilon_{xs} = u_{,s} + v_{,x} - 2zw_{,xs}$$

where subscripted commas denote partial differentiations.

Received June 6, 1990; revision received Nov. 11, 1991; accepted for publication Nov. 21, 1991.

*Research Associate, Department of Mechanical Engineering.
†Associate Professor, Department of Mechanical Engineering.